Title

Consistency in defence and competitiveness trade-off in a planktonic predator-prey system

Authors

Tom Réveillon and Lutz Becks

Affiliations

T. Réveillon (https://orcid.org/0000-0003-1788-8635) and L. Becks (https://orcid.org/0000-0002-3885-5253), Aquatic Ecology and Evolution Group, Limnological Institute, Department of Biology, University of Konstanz, Konstanz, Germany.

Data availability – Data will be uploaded on the open platform for research KonData from the University of Konstanz (https:// https://kondata.uni-konstanz.de).

Funding – This work was supported by the German Research Foundation (DFG) to LB (BE 4135/4-2) as part of the priority program "Flexibility Matters: Interplay between Trait Diversity and Ecological Dynamics Using Aquatic Communities as Model Systems – DynaTrait" (SPP 1704).

Author contributions – TR and LB compiled the first theoretical ideas. TR and LB designed the experiments. TR conducted the laboratory experiments and statistical analyses with the assistance of LB. TR wrote the initial drafts of the manuscript. TR and LB wrote the final version of the manuscript.

Acknowledgements – We are thankful to U. Gaedke for the review of an earlier version of the manuscript, to E. Ehrlich for advice on data analysis, and to R. Hermann and R. Lambrecht for the theoretical and practical contributions to the experiments.

Conflicts of interest – The authors have no conflicts of interest to declare.

Word count – Main manuscript: 9829 words. Supplementary materials: 3044 words.

Abstract

1. Predator-prey interactions play a central role in community dynamics and thus energy and matter transfers in food webs. Intraspecific variation in traits and particularly in trait combinations involved in trade-offs can alter predator-prey interactions but the underlying mechanisms governing these interactions are still unclear. Quantifying the relevant traits forming trade-off relationships and how these traits determine prey and predator fitness remains a major challenge, even for a single species. Here, we measured multiple traits related to defensive and competitive abilities to investigate the intraspecific trade-off between defence and competitiveness in 6 different strains of the green alga *Chlamydomonas reinhardtii* exposed to predation by the rotifer *Brachionus calyciflorus* and examine the consistency of the trait relationships and its consequence for the predator.

2. We found significant differences in defence and competitiveness traits that were used to categorized prey strains as defended against predation and poor competitors, undefended against predation and good competitors, or intermediate in both traits. Furthermore, we found that the different morphological and trophic traits related to defence and competitiveness of prey strains were negatively correlated. The position of prey strains in trait space were consistent independent of the defence and competitiveness trait considered. As we compared trait differences between prey strains coming from environments where selection has favoured one trait or the other, these negative correlations strongly suggested the presence of a trade-off between defence and competitiveness.

3. Our study represents the first empirical evidence of the consistency in the expression of a defence-competitiveness trade-off at the intraspecific level. Assessing the relation between relevant traits and trade-offs and understanding how it translates into fitness of prey and

49 predator allows improving general theory on the outcomes of predator-prey interactions and
50 ecosystem processes.

51 **Keywords:** fitness, defence, competitiveness, trade-off, predator-prey interactions, green algae,
52 rotifers

53

Introduction

Trophic interactions between predator and prey determine the functioning of ecosystems through their influence on population dynamics (Hudson et al. 2002; Jonsson et al. 2010), food webs (Brose et al. 2005; Petchey et al. 2008), community dynamics (Murdoch et al. 2003; Thébault and Loreau 2005) as well as fluxes of energy and matter in ecosystems (Rip and McCann 2011; Gilbert et al. 2014). For example, phytoplankton are the largest group of primary producers responsible for the acquisition and assimilation of inorganic compounds (Reynolds 2006; Halsey and Jones 2015) and herbivorous zooplankton are among the most abundant consumers of phytoplankton in aquatic ecosystems (Kiørboe 2008), transferring basal autotrophic production to higher trophic levels such as invertebrates and fishes. Thus, the trophic interaction between phytoplankton and zooplankton contributes significantly to food web dynamics and ecosystem production (Quintana et al. 2015, Turner 2015). The outcome of trophic interactions and the consequences on population dynamics are primarily determined by combinations of traits driving the performance of the interacting individuals (Colina et al. 2016). Understanding the mechanisms linking traits of phytoplankton and zooplankton to the strength of trophic interactions is therefore crucial for assessing food web functioning (Reynolds 2006; Litchman and Klausmeier 2008; Litchman et al. 2010; 2013; Edwards et al. 2013) and energy transfers between trophic levels (Turner 2002; Sommer 2008).

Traits involved in defence against predation (i.e., *sensu* grazing protection) and competitiveness (i.e., *sensu* reproduction) of phytoplankton are intimately related to the fitness of individuals and mediate trophic interactions (Colina et al. 2016). These trophic traits are often closely linked to structural traits (i.e., morphological and physiological traits). In particular, phytoplankton organisms exhibit a large variety of defence mechanisms against zooplankton grazing (Pančić and Kiørboe 2018; Lürling 2020), which interfere with different

steps of the predation sequence by preventing the encounter or the consumption by the predator (Weiss et al. 2012; Bateman et al. 2014), having either an inducible or a constitutive expression (Van Donk et al. 2011). These traits affect zooplankton predation by reducing prey detection and consumption (Rall et al. 2012) through altered attack rates (i.e., the rate of prey encounter) and the handling times (i.e., the time spent on prey manipulation) and thus have consequences on the fitness of zooplankton (Lürling and Van Donk 1996). Defence traits of phytoplankton include cell size (Long et al. 2007; Friedrichs et al. 2013), cell shape (Hessen and Van Donk 1993), cell structure (Pondaven et al. 2007; Harvey et al. 2015), life-history stage (Kolb and Strom 2013), and the formation of colonies composed of cells bound by an extracellular matrix (Verschoor al. 2004; Bernardes et al. 2021). For instance, colony formation induces an increase in handling time, which causes important reductions in ingestion and reproduction of zooplankton (Gibert and Brassil 2014).

Because organisms cannot optimize all functions contributing to fitness simultaneously due to structural (i.e., genetic) and/or functional (i.e., energetic) constraints, trade-off relationships between traits can emerge (Stearns 1989). In particular, trade-offs between defence and competitiveness are common in phytoplankton (Yoshida et al. 2004; Becks et al. 2010; Sunda and Hardison 2010; Kasada et al. 2014; Ehrlich et al. 2017; Pančić and Kiørboe 2018; Cadier et al. 2019) and may explain the diversity of defence strategies exhibited by phytoplankton (Agrawal 1998; Strauss et al. 2002). Competitiveness costs can arise from the energy investment in expressing anti-grazing defences due to a reducedability to acquire and utilize resources (Litchman et al. 2007; Halsey and Jones 2015). Indeed, cell colonies have often higher energy requirements and lower resource acquisition rates (Lürling and Van Donk 2000), which can cause a reduction in reproduction (Smith 2014). Therefore, trade-off relationships between defence and competitiveness traits can affect trophic interactions by influencing phytoplankton exploitation and zooplankton growth as well as phytoplankton

103 growth (Litchman et al. 2007; 2015; Ehrlich et al. 2020). Exploring trade-off relationships
104 between defensive and competitive abilities of phytoplankton is thus essential for understanding
105 ecological processes in planktonic communities.

106 Trade-offs between defence and competitiveness have strong implications for
107 phytoplankton communities (Ehrlich et al. 2020) and there is increasing evidence emphasizing
108 the significance of such trade-offs for trophic interactions and population dynamics (Yoshida
109 et al. 2003; 2004; Becks et al. 2010; Yamamichi et al. 2011; Kasada et al. 2014). Despite the
110 importance of trade-offs, there are few data available and the existing data should be interpreted
111 with caution. First, some studies assume fixed traits and trade-offs at the species or genus level
112 (Bruggeman 2011), but this assumption has been shown to be invalid and intraspecific variation
113 in traits can affect trophic interactions (Yoshida et al. 2004; Becks et al. 2010). Second,
114 defensive and competitive abilities of phytoplankton can be assessed by multiple traits
115 (Fleischer et al. 2018) and the relevant traits constituting trade-off are often unknown. Studies
116 use different traits as proxies for defence and competitiveness and thus different trait
117 correlations. This makes comparisons of trade-offs across studies difficult and raises the
118 question of whether different proxies can be used for studying the outcome of trophic
119 interactions. Third, negative correlations might not reflect a causal trade-off relationship due to
120 confounding factors when traits are independently affected by the same environmental
121 conditions (Edwards et al. 2011). One approach to examine the presence of trade-offs is to
122 compare trait differences between individuals originating from the same environment for which
123 selection favoured one trait and look for constrains on the other trait (Fry 2003; Fuller et al.
124 2005).

125 Determining the most suitable traits describing defence-competitiveness trade-offs and
126 information on the consistency of the trade-off relationships independent of the traits can give
127 important insights on the role for these trade-offs for energy transfers and population dynamics

128 in food webs. Here, we investigate the intraspecific trade-off relationship between anti-grazing
129 defence and competitiveness traits for 6 different prey genotypes (hereafter: strains) of the green
130 alga *Chlamydomonas reinhardtii* and evaluate the consistency of trait correlation between
131 defensive and competitive abilities of these strains (i.e., the consistent position of strains in trait
132 spaces). Furthermore, we link these traits and the resulting trade-offs to the trophic interaction
133 with the rotifer predator *Brachionus calyciflorus*. Algal strains were isolated from a previous
134 experimental evolution study and differed in their morphologies (i.e., single or colonial cells)
135 as well as defence (i.e., measured as reduction in predator growth rate) and growth (i.e.,
136 measured as strain growth rate; Bernardes et al. 2021). We measured prey defence against a
137 predator by assessing the functional response (i.e., the ingestion rate as a function of prey
138 density) and the growth rate of *B. calyciflorus* on prey strains. We measured prey
139 competitiveness by assessing the maximum growth rate and the half-saturation constant for
140 nitrate. We also measured a set of size and shape features on strains to establish a better link
141 between the prey morphology and the trophic interaction with the predator. We then used
142 parameters and rates derived from the experiments to construct and compare multiple defence-
143 competitiveness trait spaces.

Material and methods

We used 6 strains of the green alga prey *Chlamydomonas reinhardtii* (Dang 1888) derived from isolates which were originally obtained from the Chlamydomonas Resource Center (University of Minnesota, USA). Isolates were selected from monoclonal naive ancestors (i.e., no encounter with predation for thousands of generations) that were exposed or not to grazing pressure by the rotifer *Brachionus calyciflorus* for 6 months (~500 generations) in semi-continuous cultures (Bernardes et al. 2021). For the present study, a single colony from each strain was sampled from solid media and transferred to tissue culture flasks filled with 50 mL of sterile growth medium with 800 µmol NO_3^- L^{-1}. Flasks were exposed to continuous light (200 µmol photon m^{-2} sec^{-1}) and shaking (120 rpm) at 20°C for 2 weeks before assays, which allowed the cultures to reach relatively high densities. We used a clonal line of the rotifer predator *Brachionus calyciflorus* Pallas (Pallas 1766) derived from an isolate sampled in Milwaukee harbor (Bennett and Boraas 1989). This clonal line lost the ability to reproduce sexually and the possibility for evolutionary changes through genetic mixing (Fussmann et al. 2003). Rotifer stocks were kept in 1 L bottles filled with sterile growth medium with 800 µmol NO_3^- L^{-1} (Barreiro and Hairston 2013) and fed with the nutrient-rich chlorophyte alga *Monoraphidum minutum* (University of Göttingen, Germany).

Predator functional response

Prior to the experiment, *C. reinhardtii* strains were sampled from culture flasks and centrifuged at 2000 rpm for 10 min at 20 °C. The culture medium was removed and the pellets were suspended in nitrate-free medium at a density of 1×10^6 cells mL^{-1} for 24 h to significantly slow down algal growth during the exposure to predation. At the start of the experiment, strain densities were estimated and diluted to 10 different cell densities (1×10^4 to 1×10^6 cells mL^{-1}). These dilutions were made in 2 mL tubes by mixing the strain solutions with nitrate-free

medium and 200 µL were transferred into wells of 96 well plates. The experimental design included 3 replicates per cell density for each strain for the control treatment without exposure to predation to estimate the initial densities in the wells and for the predation treatment to estimate the final densities after exposure to predation. For the predation treatment, 5 adult *B. calyciflorus* were introduced per well and allowed to feed for 8 h at 20°C under continuous light. Afterwards, cells were fixated by adding 10 µL of Lugolsche solution. Plates were stored at 4°C in the dark for 24 h to allow cells to settle to the bottom of the wells. Initial and final cell densities were acquired by taking 21 images per well using a Cy5 filter set and the autofluorescence of the algal cells (642 nm) under a 10x magnification using a high content microscope (ImageXpress® Micro 4 High-Content Imaging System). Images were analyzed and cell densities were calculated using a custom module within the analysis software MetaXpress® High Content Image Acquisition and Analysis (*Supplementary Materials Appendix 1*). Ingestion rates were calculated as $I = (D_I - D_F) / (t \times R)$, where D_I is the mean initial cell density of replicate wells from the control treatment (cells mL^{-1}), D_F is the final cell density of each well from the predation treatment (cells mL^{-1}), t is the time of feeding (sec) and R is the number of rotifers per well (individuals).

Prey growth

Following the same protocol described above, *C. reinhardtii* strains were concentrated 24 h prior to the experiment. We measured growth under 9 different nitrate concentrations: 1 intermediate concentrations (100 µmol NO_3^- L^{-1}) and 6 low concentrations (1−10 µmol NO_3^- L^{-1}) to calculate half-saturation and affinity constants. At the start of the experiment, densities of strains were estimated and diluted to an initial density of 1×10^3 cells mL^{-1}. Growth assays were made in 96 well plates in a volume of 200 µL by mixing strains (20 µL) and the different nitrate-concentrated media (180 µL). We used a disruptive sampling method: a well plate was assigned to each day and cells were fixated daily in one of the replicated well plates by adding

10 µL of Lugol to the wells. The experimental design included 3 technical replicates per nitrate concentration for each strain. Plates with fixed cells were stored at 4°C in the dark for 24 h to allow cells to settle to the bottom of the wells. Cell densities were assessed as described above and growth curves were estimated over 8 days.

Predator growth

C. reinhardtii strains were sampled from culture flasks and diluted to 5×10^5 cells mL^{-1} in 1 mL of a nitrate-free medium in 24 well plates. The nitrate-free medium and the moderate initial cell density allowed for the control of prey population only by the predator during the experiment and provided sufficient resource over time for the predator while preventing stress for the predator due to foraging in saturating resource conditions (personal observation). We added 2 juveniles and 3 adult rotifers carrying 1 or 2 eggs to the wells to maintain a homogeneous age structure in the initial population. The experimental design included 5 replicates for each strain. Rotifer individuals were daily counted using a stereomicroscope and growth curves were estimated over 5 days.

Prey morphology

To assess the variation in morphological traits among and within *C. reinhardtii* strains, 100 µL was sampled from the culture flasks of *C. reinhardtii* strains and transferred into 1.5 mL tubes. Samples were mixed using a vortex at 1000 rpm and imaged using an imaging flow cytometer (Amnis® ImageStreamX Mk II). A collection of 5000 images was acquired for each strain with a 20X magnification using the red channel (642 nm) and the autofluorescence of algal cells for image acquisition. A selection of 40 morphological features (Tab. S1) was calculated per image using a related analysis software (Amnis IDEAS®, see *Supplementary Materials Appendix 2*). We used these features to characterize morphological differences between strains (i.e., inter-strain clustering) and within strains (i.e., intra-strain clustering). Cell morphotypes within

strains were classified by the number of cells present in each image and divided in 4 categories: single (1 cell), small clump (2−5 cells), medium clump (6−10 cells) and large clump (10−30 cells). The number of cells was calculated based on a ratio A_i / A_r, where A_i is the area of a single cell or cell clump i (µm^2) and A_r is the mean area of a single cell (136 µm^2) based on a strain exhibiting only single cells (C_{R4}). A_r was calculated following the removal of values below and above the confidence interval boundaries ($CI_{2.5\%}$−$CI_{97.5\%}$).

Statistical analyses

To estimate predator functional responses, the mean ingestion rate of the 3 replicates was calculated over the range of cell densities for each *C. reinhardtii* strain. Following the disc equation (Holling 1959), functional responses were expressed as mean ingestion rate of the predator (I_i) as a function of prey densities (A_i) and predator ingestion parameters. A selection of 4 functional response models were compared to assess the best representation of data (Tab. S1). We chose the widespread Holling types I, II and III models (Holling 1965) along with the Ivlev type II model (Ivlev 1955). The Holling type I represents a linear increase of ingestion rate while the Holling type II and type III exhibit a non-linear increase of ingestion rate, which reaches a saturation at high prey density. The Ivlev type II is considered equivalent to the Holling type II but defined with different functional parameters. We fitted the 4 functional response models for each strain using non-linear least squares regressions and compared them with likelihood ratio tests (Tab. S2). We then selected the best fitting strain-specific models to estimate ingestion rate over prey densities, which was the Holling type II model (Eq. 1):

$$I_i = \frac{a_i A_i}{1 + a_i h_i A_i} \qquad \text{(Eq. 1)}$$

where a_i is the attack rate of the predator on strain i (mL sec^{-1}), h_i is the handling time of the predator on strain i (sec^{-1}) and A_i is the cell density of strain i (cells mL^{-1}). Using the fitted

parameters from the previous model (Eq. 1), ingestion rates were predicted over a larger range of cell densities than in the experiment (up to 1.5×10^6 cells mL^{-1} with a 0.1 step) to better fit the functional response curvatures at high cell densities (i.e., ingestion saturation) and obtain comparable curves among strains. Then, we estimated strain-specific attack rates as the slopes of ingestion rate at low prey densities (5×10^5 cells mL^{-1}) and strain-specific handling times as the maximum ingestion rates at high prey densities (1.5×10^6 cells mL^{-1}). To further describe anti-grazing defences of prey strains, we also estimated strain-specific detection and ingestion probabilities by the predator as proposed by Ehrlich and Gaedke (2018) following a modified expression of Holling type II model (Eq. 2):

$$I_i = \frac{a d_i p_i A_i}{1 + a h d_i A_i} \qquad \text{(Eq. 2)}$$

where a is the species attack rate of the predator (mL sec^{-1}), h is the species handling time of the predator (sec^{-1}), d_i is the detection probability of strain i (i.e., probability for the predator to detect the prey), p_i is the ingestion probability (i.e., probability for the predator to consume the detected prey) and A_i is the cell density of strain i (cells mL^{-1}) (*Supplementary Materials Appendix 3*).

To estimate prey growth rates, the mean cell density of the 3 replicates was calculated over the range of nitrate concentrations for each *C. reinhardtii* strain and day. A selection of 5 growth models were compared following the approach of Paine et al. (2012) to assess the best representation of data (Tab. S2). We chose 2 non-asymptomatic models which assume of an unlimited cell growth over time: a linear model, representing a constant increase in cell density over time and an exponential model for a disproportional increase in cell density over time. We also chose 3 asymptomatic models which make the assumption of a limited cell growth with a maximum cell density reached over time: a monomolecular model describing a vertical increase in cell density which reaches rapidly an horizontal asymptote (i.e., maximum population cell

density), a logistic model describing a slow increase in cell density with an inflection point (i.e., time point for maximum growth rate) around 50% of the asymptotic cell density and a Gompertz model describing a rapid increase in cell density with an inflection point around 37% of the asymptotic cell density (Heinen 1999). We fitted the 5 growth models to each combination of strain and nitrate treatment using non-linear least squares regressions on log-transformed cell densities and we compared them with likelihood ratio tests (Tab. S3). We then selected the best fitting strain-specific model to estimate cell density over time, which was the logistic model (Eq. 3):

$$D_i = \frac{b_i K_i}{b_i + (K_i - b_i)e^{-r_i t}} \quad \text{(Eq. 3)}$$

where b_i is the initial cell density of strain i (cells mL^{-1}), K_i is the asymptotic cell density of strain i (cells mL^{-1}), r_i is the intrinsic growth rate of strain i (cells day^{-1}) and t is the time (day^{-1}). Using the fitted parameters from the previous model (Eq. 3), cell densities were predicted over a larger range of days than in the experiment (up to 10 days with a 0.1 step) to better fit the growth curvatures at high cell densities (i.e., growth saturation). *Per capita* growth rates were also calculated for each strain and nitrogen concentration using linear regressions over the full time series (i.e., over 10 days) to obtain the overall *per capita* growth rate (G) and for each 3 consecutive time steps (i.e., each 0.3 days) to find the maximum per capita growth rate (G_m). Then, we estimated strain-specific half-saturation and affinity constants for nitrate using non-linear least squares regressions on the Monod equation (Monod 1950):

$$G_i = G_{mi}\frac{N}{K_i + N} \quad \text{(Eq. 4)}$$

where G_i is the overall *per capita* growth rate of strain i (day^{-1}) G_{mi} is the maximum *per capita* growth rate of strain i (day^{-1}), K_i is the half-saturation constant of strain i (µmol NO_3^- L^{-1}) and N is nitrate concentration (µmol NO_3^- L^{-1}). Affinity constants were calculated as $A_i = G_{mi} / K_i$,

where G_{mi} is the maximum *per capita* growth rate of strain *i* (day^{-1}) among all nitrate concentrations and K_i is the half-saturation constant of strain *i* (µmol NO_3^- L^{-1}).

To estimate predator growth rates, the mean *B. calyciflorus* density of the 5 replicates was calculated for each *C. reinhardtii* strain and day. A selection of 4 growth models were compared to assess the best representation of data (Tab. S3) depending on the response of the rotifer populations to different prey strains. We chose a linear model, an exponential model, a logistic model (Eq. 3) and a mortality model (Eq. 5) describing an increase or a stabilization and then a decrease in rotifer density (Malerba et al. 2018). We fitted the 4 growth models using non-linear least squares regressions on rotifer densities and we compared them with likelihood ratio tests (Tab. S4). We then selected the best fitting strain-specific model to estimate rotifer density over time, which was the mortality model for strains C_{R1}, C_{R2}, C_{R3} and C_{R4} (Eq. 3) and the logistic model for strains C_{R6} and C_{R7} (Eq. 5):

$$D_i = K_i e^{m_i(t-t_{mi}) - \frac{m_i}{r_i}\left(1-e^{-r(t-t_{mi})}\right)} \quad \text{(Eq. 5)}$$

where r_i is the intrinsic growth rate of rotifer for strain *i* (ind day^{-1}), K_i is the asymptotic rotifer density for strain *i* (ind mL^{-1}), m_i is the decreasing slope following maximum rotifer density for strain *i* (ind day^{-1}), *t* is the time (day^{-1}) and t_{mi} is the time for maximum intrinsic growth rate of rotifer for strain *i* (day^{-1}). *Per capita* growth rates were also calculated for each strain using linear regressions over the full time series (i.e., over 5 days).

A principal components analysis (PCA) was conducted on the 40 morphological features estimated on collections of individual cell images. Features chosen for this analysis were divided in 2 categories: cell size for traits over 1 dimension and cell shape for traits over 2 dimensions. The PCA was run on the image collections containing 30000 images (5000 images per strain) and the 2 first dimensions explaining most of the variance in the data were selected (D_1 = 46.5%, D_2 = 19.9%). Coefficients of variation (CV) were calculated for each of

the 40 features for each strain as CV = (sd_x / m_x) × 100, where sd_x and m_x are the standard deviation and the mean of feature *x*, respectively. In addition, pairwise correlations between the relevant features Area (size) and Circularity (shape) according to contributions to the PCA dimensions were performed using linear regressions and Pearson correlation tests. Statistical differences in these two relevant morphological features among strains and among morphotypes within strains were also tested using Kruskal-Wallis and Dunn post-hoc tests.

Statistical analyses were computed using the R software v.4.0.4 (R Development Core Team 2020). The principal components analysis was computed using the *PCA* function from the 'FactoMineR' R package. Linear regressions and non-linear least squares regressions were computed using the *lm* and *nls* functions from the 'lme4' R package. Models were compared using the *lrt* function from the 'lmtest' R package and significance was obtained using the *anova* function from the 'stats' R package.

Results

Predator functional response

The defence of *C. reinhardtii* strains was defined based on the ingestion rate of the predator *B. calyciflorus* and ranged from defended (low ingestion) to undefended (high ingestion). The comparison of functional response models revealed that the ingestion rates of *B. calyciflorus* on *C. reinhardtii* strains were better described by non-linear saturating models (Tab. S1, Fig. S1a). *B. calyciflorus* ingestion rates differed among strains and depended on cell densities (Fig. 1a). Strains C_{R1}, C_{R2} and C_{R3} were classified as defended due to the low maximum ingestion rates exhibited by the predator (e.g., C_{R1}: 0.43 ± 0.09 and C_{R2}: 0.49 ± 0.11 cells sec^{-1} mL^{-1} ind^{-1}) while intermediate strains C_{R6} and C_{R7} were considered as due to the moderate maximum ingestion rates exhibited by the predator (e.g., C_{R6}: 1.32 ± 0.10 and C_{R7}: 1.19 ± 0.12 cells sec^{-1} mL^{-1} ind^{-1}). In contrast, strain C_{R4} was classified as undefended due to the high maximum ingestion rates exhibited by the predator (3.41 ± 0.26 cells sec^{-1} mL^{-1} ind^{-1}), which was characterized by a saturation plateau appearing at very high prey density (> 1.5×10^6 cells mL^{-1}). These differences in the shapes of the functional responses were confirmed by a large variation in functional parameters: *B. calyciflorus* expressed lower attack rates (e.g., C_{R1}: 0.06 ± 0.01 against C_{R4}: 0.46 ± 0.07 mL sec^{-1}) but higher handling times (e.g., C_{R1}: 2.84 ± 0.36 against C_{R4}: 0.35 ± 0.02 sec^{-1}) on defended strains compared to undefended strains. Moreover, we calculated detection and ingestion probabilities as proxies for anti-grazing defences of strains (Tab. 1). Defended strains had variable detection probabilities (e.g., C_{R1}: 0.41 and C_{R2}: 1.00) but consistently low ingestion probabilities (e.g., C_{R1}: 0.12 and C_{R2}: 0.16) whereas undefended strains also had variable detection probabilities (e.g., C_{R4}: 0.44 and C_{R6}: 0.79) but consistently high ingestion probabilities (e.g., C_{R4}: 1.00 and C_{R6}: 0.45).

Prey growth

The competitiveness of *C. reinhardtii* strains was classified based on the growth rate and ranged from non-competitive (low growth) to competitive (high growth). The comparison of growth models revealed that the growth curves of *C. reinhardtii* strains were better described by a non-linear logistic model (Tab. S2, Fig. S1b). Growth rates differed among *C. reinhardtii* strains and showed the same grouping as for ingestion rate (Fig. 1b). Defended strains C_{R1}, C_{R2} and C_{R3} were classified as non-competitive due to the low maximum cell densities (e.g., C_{R2}: 0.76 ± 0.27 and C_{R3}: 0.64 ± 0.28 10^5 cells mL^{-1}) and low *per capita* growth rates (e.g., C_{R2}: 0.08 ± 0.01 and C_{R3}: 0.09 ± 0.01 day^{-1}) while intermediate and undefended strains C_{R4}, C_{R5} and C_{R6} were classified as competitive due to the high maximum cell densities (e.g., C_{R4}: 5.22 ± 0.95 and C_{R6}: 5.02 ± 1.12 10^5 cells mL^{-1}) and high *per capita* growth rates (e.g., C_{R4}: 0.21 ± 0.01 and C_{R6}: 0.22 ± 0.02 day^{-1}). Furthermore, nutrient acquisition rates differed among *C. reinhardtii* strains (Fig. 1c). Defended strains had low nitrate affinities (e.g., C_{R2}: 0.15 ± 0.07 µmol NO_3^- L^{-1} day^{-1}) and high half-saturation constants (e.g., C_{R2}: 1.43 ± 0.35 µmol NO_3^- L^{-1}) whereas undefended strains had high nitrate affinities (e.g., C_{R4}: 1.26 ± 0.23 µmol NO_3^- L^{-1} day^{-1}) and low half-saturation constants (e.g., C_{R4}: 0.37 ± 0.04 µmol NO_3^- L^{-1}).

Predator growth

Defensive and competitive abilities of *C. reinhardtii* strains had an impact on the population dynamic of the predator beyond reducing the maximum predator population density (Fig. 1d). The comparison of growth models revealed that *B. calyciflorus* exhibited a logistic growth in the presence of intermediate defended strains (C_{R6} and C_{R7}) but logistic growth followed by a decline in the presence of defended (C_{R1}, C_{R2} and C_{R3}) and undefended (C_{R4}) strains. Defended strains were associated with lower maximum predator densities (e.g., C_{R2}: 12.26 ± 0.29 and C_{R3}: 12.09 ± 0.36 ind mL^{-1}) and lower *per capita* growth rate (e.g., C_{R2}: 0.96 ± 0.18 and C_{R3}: 0.94 ± 0.18 day^{-1}) while intermediate defended strains were associated with higher maximum predator densities (e.g., C_{R6}: 19.51 ± 0.17 and C_{R7}: 28.41 ± 0.91 ind mL^{-1}) and higher *per capita*

372 growth rates (e.g., C_{R6}: 3.33 ± 0.13 and C_{R7}: 5.47 ± 0.12 day^{-1}). Interestingly, the undefended
373 strain (C_{R4}) was associated with a rapid increase followed by a decrease in predator density
374 (from 17.76 ± 0.84 to 13.75 ± 3.74 ind mL^{-1}) and *per capita* growth rate (from 4.78 ± 0.13 to
375 −2.43 ± 0.12 day^{-1}), suggesting prey limitation leading to the decline of the predator population.

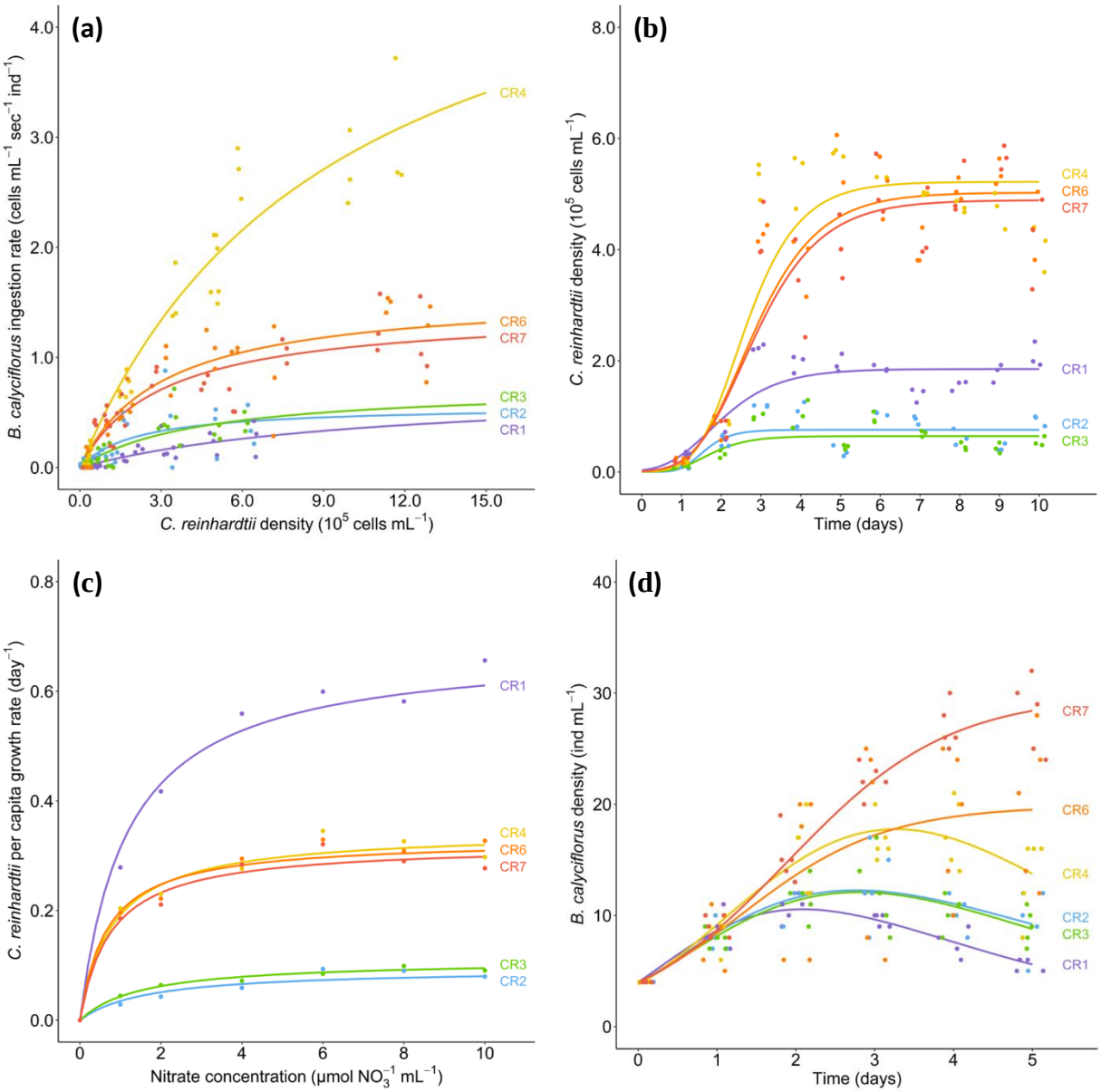

376 **Figure 1:** (a) Functional responses of *B. calyciflorus* showing ingestion rate as a function of
377 cell density of *C. reinhardtii* strains. Predicted functional response curves (lines) were estimated
378 from 3 replicates (symbols). (b) Growth curves of *C. reinhardtii* strains shown as cell densities
379 over time for an intermediate nitrate concentration (100 µmol NO_3^- L^{-1}). Predicted growth
380 curves (lines) were estimated from 3 replicates (symbols). (c) Growth rate of *C. reinhardtii*
381 strains over nitrate concentrations (1−10 µmol NO_3^- L^{-1}). All Predicted curves were calculated
382 using the mean *per capita* growth rate (dots). (d) Growth curves of *B. calyciflorus* feeding on
383 *C. reinhardtii* strains shown as rotifer densities over time. Predicted growth curves (lines) were
384 estimated from 3 replicates (symbols).

385 *Prey morphology*

386 To investigate whether the observed differences in defensive and competitive abilities of *C.*
387 *reinhardtii* strains were related to morphological differences among strains, we analysed
388 morphological traits in more detail. Strains exhibiting strong clumping morphologies (C_{R1}, C_{R2}
389 and C_{R3}) displayed populations covering a larger spectrum of the PCA dimensional space (Fig.
390 2a) compared to strains exhibiting mostly single cell morphologies (C_{R4}, C_{R6} and C_{R7}).
391 Clumping strains were positively correlated to traits indicating large asymmetric cell aggregates
392 (e.g., contributions on D_1: Area = 0.21 and Asymmetry = 0.17, Fig. 2b) and negatively
393 correlated to traits indicating small symmetric cell sizes (e.g., contributions on D_1: Circularity
394 = −0.14 and Sphericity = −0.19, Fig. 2b).

395 Accordingly, relevant morphological features with high contributions in the PCA were
396 significantly different among strains (e.g., Area: Kruskal-Wallis, χ^2 = 8177.60, P < 0.001)
397 Clumping strains exhibited on average larger sizes (e.g., Area ± standard deviation: C_{R1}: 323 ±
398 230 µm; C_{R4}: 108 ± 35 µm, Fig. 3a) and less symmetric shapes (e.g., Circularity: C_{R1}: 11.78 ±
399 7.80 and C_{R4}: 19.11 ± 5.24, Fig. 3a). Moreover, clumping strains exhibited a larger diversity of
400 cell morphotypes within population ranging from single cells to large cells aggregates (Fig. 2a
401 and 3a). The 40 CV of morphological features were significantly different among strains (i.e.,
402 inter-strain variance, Kruskal-Wallis, χ^2 = 20.64, P < 0.001) with higher mean CV values for
403 clumping strains (e.g., C_{R1}: 46% and C_{R4}: 32%, Fig. 3b). Moreover, the 40 CV were
404 significantly different among morphotypes only within clumping strains (i.e., intra-strain
405 variance, e.g., C_{R2}: Kruskal-Wallis, χ^2 = 16.39, P < 0.001 and C_{R6}: Kruskal-Wallis, χ^2 = 0.36,
406 P = 0.551). These observations suggest that clumping strains consisted of distinct subclasses of
407 cell morphotypes. Overall, the presence or absence of clumping morphotypes coincided with
408 the defensive and competitive abilities of strains, meaning that strains having large cell clumps
409 were characterized as very defended and poorly competitive and vice versa (Fig. 4).

410

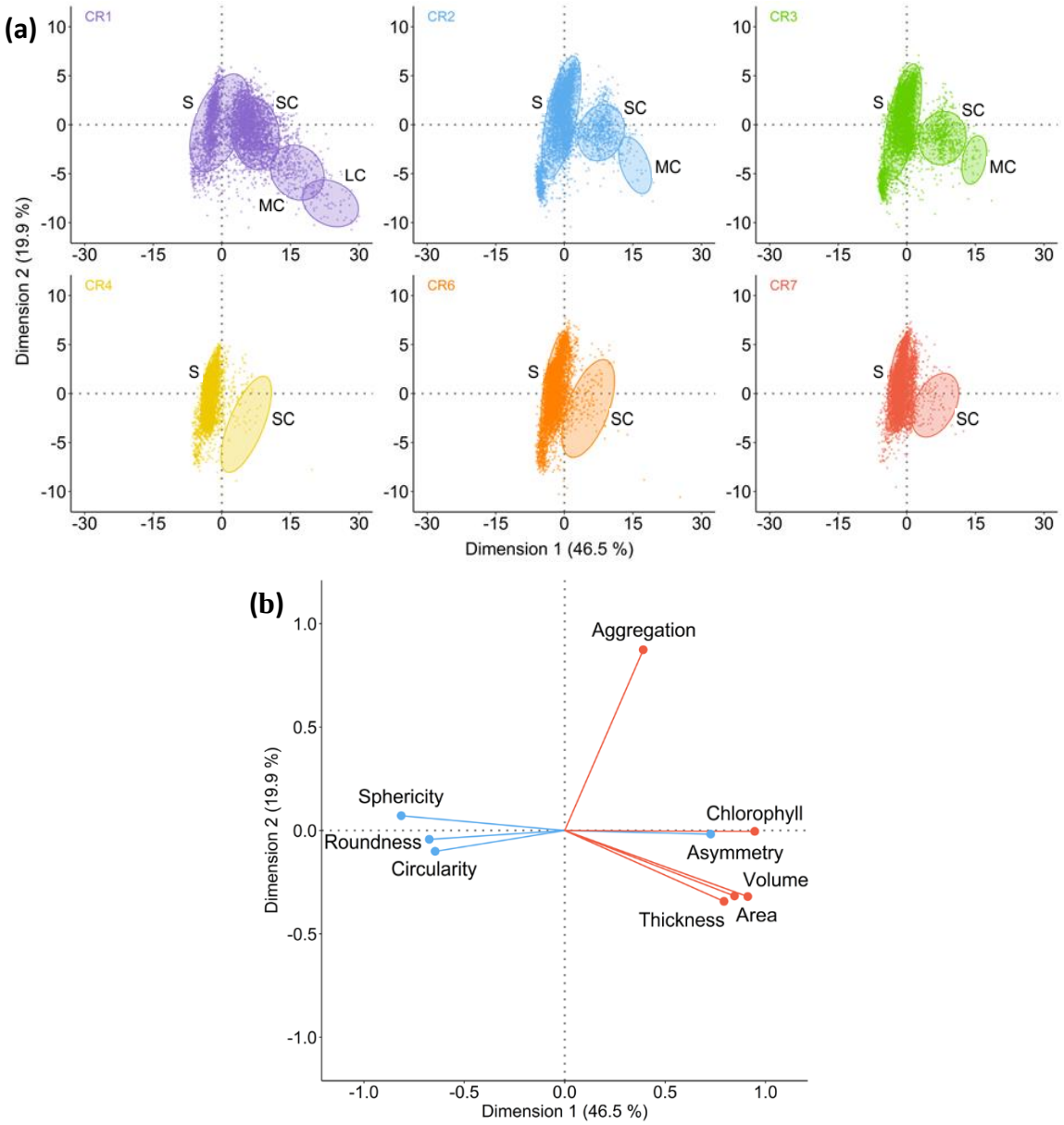

411 **Figure 2:** (a) Representation of the principal components analysis (PCA) showing (a) the
412 position of individual cell observations for populations of C. reinhardtii strains (n = 5000) and
413 (b) the positions of the most representative morphological features (n = 9) along the 2 main
414 dimensions explaining most of the variance (D1 = 46.5% and D2 = 19.9%). Ellipses group 95%
415 of the cell observations for each morphotype population within strains. Morphotype categories:
416 single cell (S, 1 cell), small clump (SC, 2−4 cells), medium clump (MC, 5−10 cells) and large
417 clump (LC, > 10 cells). Features represented here were selected based on the highest
418 contributions to the 2 main dimensions according to the PCA and were divided in 2 groups:
419 size features (red) and shape features (blue).

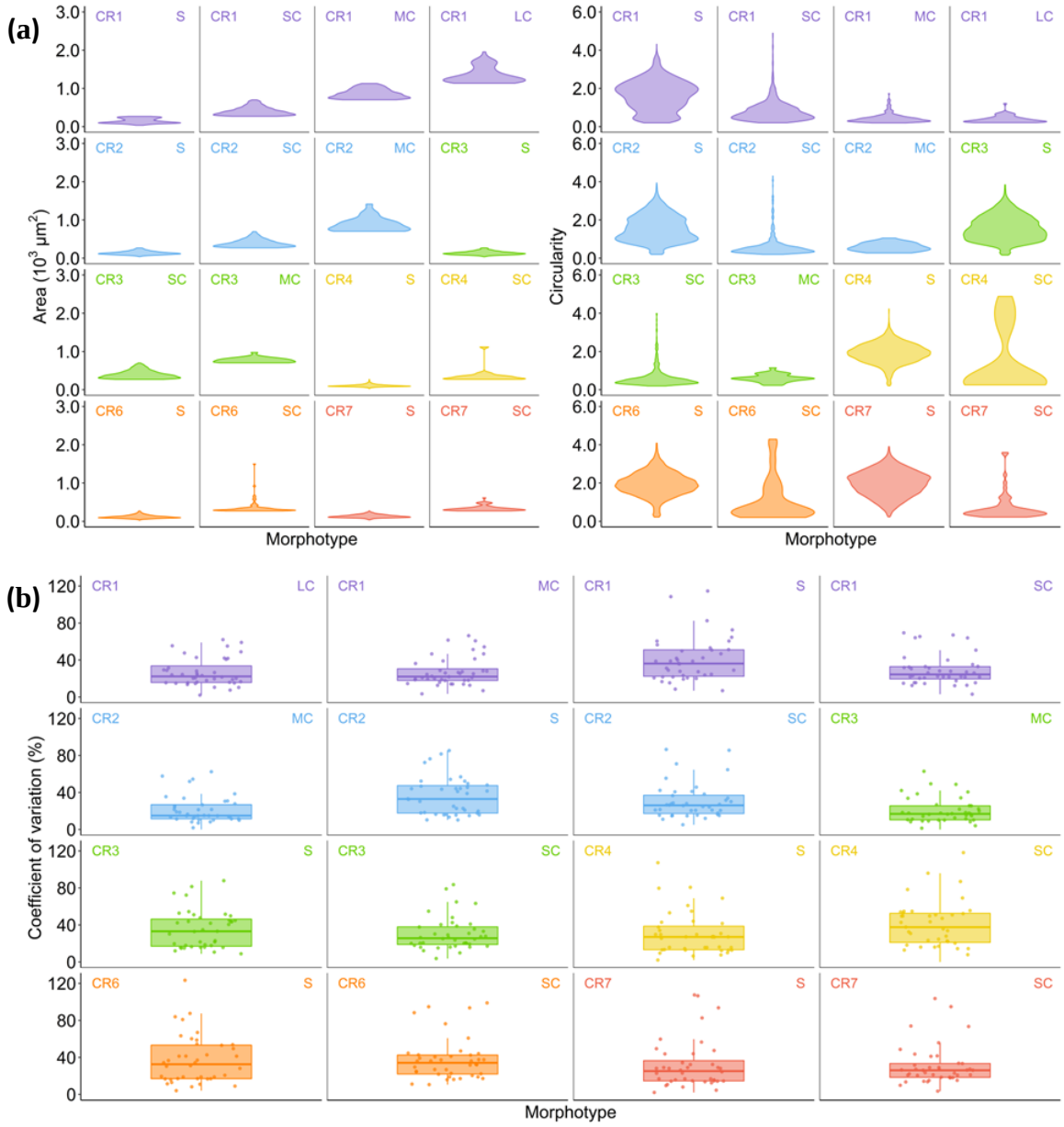

Figure 3: (a) Density distribution of values for 2 relevant morphological features (Area for size and Circularity for shape) explaining most of the variance in the PCA for each *C. reinhardtii* morphotype population. (b) Distribution of coefficients of variation for morphological traits of the PCA (n = 40 traits) for each *C. reinhardtii* morphotype with median and quartiles (boxes) and 95% confidence intervals (vertical bars). Morphotype categories: single cell (S, 1 cell), small clump (SC, 2−4 cells), medium clump (MC, 5−10 cells) and large clump (LC, > 10 cells).

427 *Defence-competitiveness trade-off*

428 The relationship between anti-grazing defence and competitiveness traits of *C. reinhardtii*
429 strains was consistent for the different traits we used (Fig. 4a). Defended and non-competitive
430 strains (C_{R1}, C_{R2} and C_{R3}) were positioned on the top left corner of the trait space, being
431 characterized by large-sized cell clumps (e.g., C_{R1}: 323 ± 230 µm), resulting in low attack rates
432 (e.g., C_{R1}: 0.06 ± 0.01 mL sec^{-1}), high handling times (e.g., C_{R1}: 2.84 ± 0.36 sec^{-1}) and low
433 growth rates for the predator (e.g., C_{R1}: −0.05 ± 0.18 day^{-1}). Conversely, undefended and
434 competitive strains (C_{R4}, C_{R6} and C_{R7}) were positioned on the bottom right corner of the trait
435 space, being characterized by small-sized single cells (e.g., C_{R4}: 108 ± 35 µm), resulting in high
436 attack rates (e.g., C_{R4}: 0.46 ± 0.07 mL sec^{-1}), low handling times (e.g., C_{R4}: 0.35 ± 0.02 sec^{-1})
437 and high growth rates for the predator (e.g., C_{R4}: 2.33 ± 0.27 day^{-1}). Moreover, the positions of
438 strains were similar for trait spaces constructed with prey growth rates or nutrient acquisition
439 rates (i.e., nitrate affinities and half saturation constants) as traits for competitiveness (Fig. 4b).
440 Furthermore, the variance in anti-grazing defence and competitiveness traits within strains was
441 low or moderate so that most of the strain-specific surfaces covered on the trait spaces (i.e.,
442 standard deviations) were not overlapping, reinforcing the relevance of these traits for
443 predicting different fitness strategies.

444

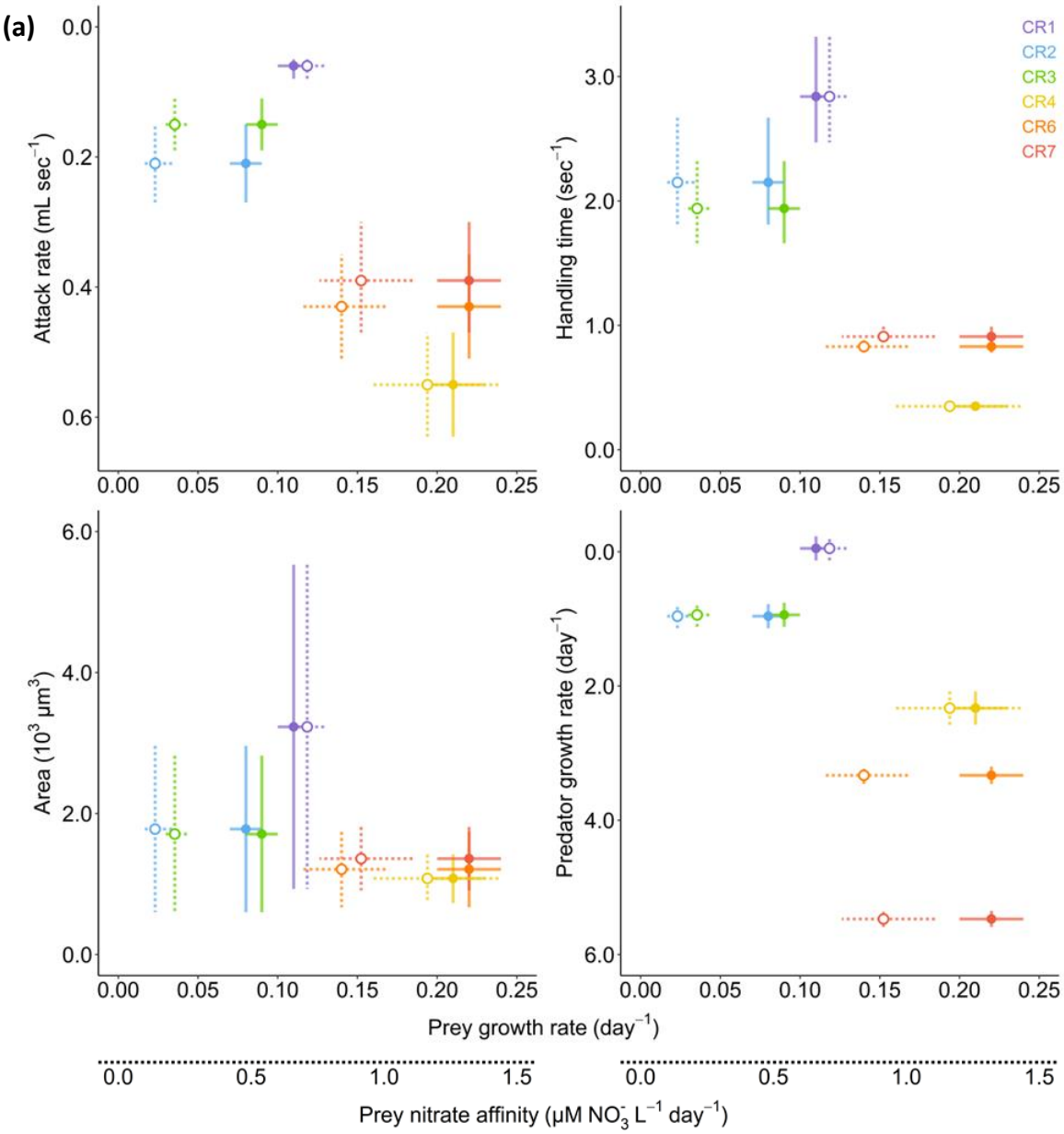

445

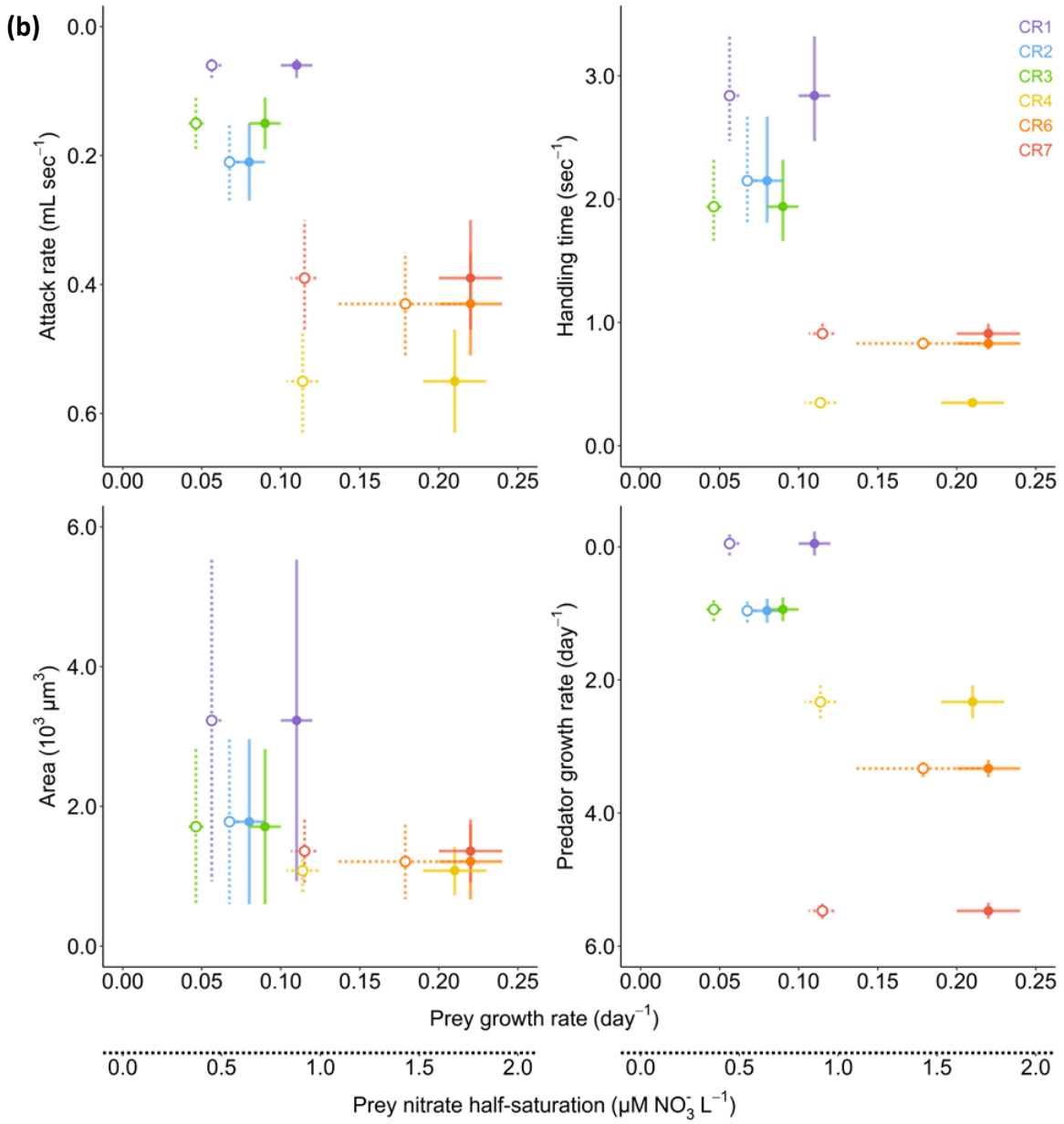

446 **Figure 4:** Defence-competitiveness trait spaces showing the positions of *C. reinhardtii* strains
447 for 4 anti-grazing defence traits (i.e., attack rate, handling time, cell area and predator *per capita*
448 growth rate) as a function of 3 competitiveness traits (i.e., prey *per capita* growth rate, nitrate
449 affinity constant and nitrate half-saturation constant). Trait values (symbols) and standard
450 deviations (horizontal and vertical bars) were represented pairwise for competitiveness traits on
451 each plot: (a) growth rate (filled symbols and solid bars) and nitrate affinity constant (open
452 symbols and dotted bars) and (b) growth rate (filled symbols and solid bars) and nitrate half-
453 saturation constant (open symbols and dotted bars). Values of attack rate and predator *per*
454 *capita* growth rate were flipped to orientate the axis according to the trade-off hypothesis:
455 increasing defence (y-axis) against increasing competitiveness (x-axis).

Discussion

Exploring the intraspecific variation in traits related to fitness in phytoplankton species, such as defence against zooplankton grazing and competitiveness, is essential to understand fitness strategies and predict ecological interactions of planktonic species (Hairston et al. 2005). We found substantial variation in trophic and morphological traits related to anti-grazing defence and competitiveness for 6 different strains of *C. reinhardtii*. The patterns of variation were consistent for the different defence and competitiveness traits as *C. reinhardtii* strains had similar positions when comparing in trait space. Moreover, we identified a consistent negative relationship between defence and competitiveness traits, suggesting a limitation in energy investment between these two fitness components (Stearns 1989). The consistency of the trade-off relationship confirmed that multiple morphological and trophic traits of prey and predator can constitute suitable proxies to assess prey fitness strategies and the strength of predator-prey interaction. Measuring consistent indicators for defence-competitiveness trade-offs could be particularly relevant for the assessment of ecological dynamics in disturbed ecosystems because direct and indirect (i.e., via interacting species) responses of species depend on the presence (Yamamichi and Miner 2015) and the amount of trait variation (Hermann and Becks 2022). In addition, the heritability of trait variation represents a prerequisite for adaptation of species to disturbed ecosystems and this depends to a large extent on trade-offs (Smith et al. 2016).

Prey defence against predation was well estimated using prey morphology, predator ingestion or predator growth. Morphological traits are particularly relevant to estimate the variation in defensive abilities among and within prey population and can serve as good indicators of changes in the defence trait of prey population over time in both empirical (e.g., Becks et al. 2010) and modelling studies (e.g., Ellner and Becks 2011). Some caution is still required with morphology as other structural traits related to physiology and behaviour which

480 we did not consider can contribute to defence (Pančić and Kiørboe 2018; Lürling 2020). Prey
481 competitiveness was well estimated using prey growth and resource acquisition, which shows
482 a relation between the processes of nutrient absorption, assimilation, and conversion to
483 reproduction (Litchman et al. 2007). However, complex interplays between processes may
484 complicate predictions as prey competitiveness can also be driven by other regulating factors
485 such as the acquisition of colimiting resources (Klausmeier et al. 2004) or trade-offs between
486 nutrient and light acquisition (Strzepek and Harrison 2004).

487 Developing empirical methods that examine the consistency of the relationship between
488 traits is central to confirm the presence of trade-offs. We used 6 isolates of *C. reinhardtii*
489 selected from monoclonal populations that grew in the presence or absence of predation by *B.*
490 *calyciflorus* (Bernardes et al. 2021). Our approach circumvents some difficulties of previous
491 studies examining suitable indicators as we measured trade-offs using clones derived from a
492 selection experiment where monoclonal ancestors evolved in different environments in which
493 selection either favoured defence or competitiveness (Bernardes et al. 2021). This approach has
494 been proven to be more suitable for detecting trade-offs (Kassen 2002; Fry 2003; Fuller et al.
495 2005) because negative correlations between traits measured in clones isolated from the same
496 environment or from different environments without assessing the environmental conditions
497 are not evidence of evolutionary constraint (Stearns 1989). Similarly, a positive or no
498 correlation can result from several confounding factors (e.g., small detection signal or
499 environmental conditions) and thus does not imply causality or lack thereof (Bohannan et al.
500 2002; Fry 2003). To our knowledge, our study is the first to extend the characterization of clonal
501 lines to multiple traits to examine the consistency of an intraspecific trade-off between defence
502 and competitiveness using evolved isolates for which the history of selection is known.

503 Algal prey strains considered as defended against ingestion by the predator were
504 growing as clumped cells bound by a viscous extracellular matrix which colony sizes of 10−30

505 cells. These strains were associated with lower functional responses of the predator, which were
506 mainly the consequence of a longer handling time and the inability of the predator to ingest cell
507 colonies. Colony formation can be an effective defence for phytoplankton and significantly
508 reduces zooplankton grazing (Van Donk et al. 1999; Reynolds 2006). Palmelloid colonies were
509 previously observed for *C. reinhardtii* in the presence of the rotifer *B. calyciflorus* and was
510 shown to be due toeither from phenotypic plasticity (i.e., inducible, Lürling 2006; Fischer et al.
511 2014) or adaptive evolution (i.e., constitutive, Becks et al. 2010; Ratcliff et al. 2013; Bernardes
512 et al. 2021). Palmelloid colonies are composed of cells forming large aggregates (~10−120
513 cells) embedded in an extracellular matrix (Lürling 2006). In addition to colonies reducing
514 ingestion rates of gape size limited predators, the extracellular matrix can also provide a
515 digestion resistance to cells during gut passage (Van Donk and Hessen 1993; DeMott et al.
516 2010). Furthermore, we found substantial variation in competitiveness traits among the 6
517 different strains of *C. reinhardtii*. Prey strains considered as competitive were associated with
518 higher nitrate affinities and *per capita* growth rates and lower nitrate half-saturation constants,
519 which indicated enhanced abilities for nutrient acquisition and/or conversion to reproduction
520 (Litchman et al. 2007; Litchman and Klausmeier 2008; Halsey and Jones 2015; Ward et al.
521 2017). Competitive abilities of phytoplankton species mainly depend on surface-area constrains
522 in terms of resource acquisition and requirements for basal maintenance and functions
523 contributing to fitness. Single cells tend to have higher nutrient acquisition rates due to a more
524 efficient diffusion of molecules (Yoshiyama and Klausmeier 2008) while palmelloid colonies
525 are more limited by nutrient and light competition among colonial cells and a shading effect
526 (Raven and Kubler 2002), despite larger nutrient storage capacities (Litchman et al. 2009).

527 Intraspecific variation in trophic and morphological traits of preys is expected to have
528 important consequences on higher trophic levels and ecosystem functioning. We found that the
529 numerical response of the predator *B. calyciflorus* differed depending on the defensive and

competitive abilities of *C. reinhardtii* strains. Predator populations were increasing and then decreasing in the presence of defended prey strains but were increasing more and then constant in the presence of intermediate and competitive prey strains. Such observations suggest a mechanistic link between prey defensive and competitive abilities, predator-prey trophic interactions and predator reproduction (Litchman et al. 2013). Moreover, defence and competitiveness traits of phytoplankton are fundamental determinants of the energy intake by zooplankton predators by defining food quantity and quality (Bi and Sommer 2020). Prey defensive morphologies and stochiometric ratios might reduce food quality, which prevents the predator from meeting its biochemical requirements and thus reduces its survival and reproduction (Sommer et al. 2012). The considerable impact of prey fitness on predator fitness, driven by a defence-competitiveness trade-off, and the implications for energy transfers between trophic levels highlights the importance of assessing the consistency of trade-offs to determine the outcome of trophic interactions and food web dynamics.

Investigating intraspecific trade-off relationships between defensive and competitiveness traits is fundamental to understand fitness strategies of phytoplankton (Litchman et al. 2007; Cadier et al. 2019; Ehrlich et al. 2017) and estimate the strength of trophic interactions and coexistence between phytoplankton and zooplankton species (Våge et al. 2014; Cadier et al. 2019; Ehrlich et al. 2020). Our study demonstrates the consistency of an intraspecific defence-competitiveness trade-off relationship estimated empirically over a broad range of trophic traits measured on both prey and predator organisms. Previous studies have shown that intraspecific trade-off relationships are a prerequisite for eco-evolutionary feedback dynamics, which in turn contribute to the maintenance of trait variation (e.g., Becks et al. 2010; 2012; Kasada et al. 2014). Knowledge on the underlying traits involved in trade-offs and how these trade-offs translate into fitness of organisms at different trophic levels is required for predicting the response of communities to environmental perturbation (Jessup and Bohannan

555 2008; Frickel et al. 2017; Theodosiou et al. 2019; Hermann and Becks 2022). The comparisons
556 of trait variation and trade-offs at the intra- and interspecific levels (Ehrlich et al. 2017; 2020)
557 could also provide key insights into the role of intraspecific diversity and trade-offs for species
558 coexistence and ecosystem functioning with environmental change.

559

Tables

Table 1: Functional parameters [± standard deviation] of the 6 different *C. reinhardtii* strains. Anti-grazing defences were represented by the attack rate (*a* in mL sec^{-1}), the handling time (*h* in sec^{-1}), the detection probabilities (*p*) and the ingestion probabilities (*d*). Competitiveness ability was represented by the half-saturation constants (*K* in µmol NO_3^- L^{-1}) and the affinity constants (*A* in 10^3 µmol NO_3^- L^{-1} day^{-1}) for nitrate. Strains exhibited different morphologies in terms of cell clumping: clumping strains were C_{R1} (large free clumps [10−30 cells]), C_{R2} (medium mucous clumps [5−10 cells]), C_{R3} (medium mucous clumps [5−10 cells]) and C_{R7} (small free clumps [3−5 cells]) while non-clumping strains were C_{R4} (small single cells, motile) and C_{R6} (small single cells).

Strain	*a*	*h*	*p*	*d*	*K*	*A*
C_{R1}	0.06 [0.05−0.08]	2.84 [2.47−3.32]	0.35 [0.39−0.44]	0.12 [0.11−0.14]	0.92 [0.85−0.98]	0.77 [0.72−0.84]
C_{R2}	0.21 [0.15−0.27]	2.15 [1.81−2.67]	1.00 [1.00−1.00]	0.16 [0.14−0.19]	1.43 [1.09−1.78]	0.15 [0.10−0.22]
C_{R3}	0.15 [0.11−0.19]	1.92 [1.63−2.34]	0.65 [0.64−0.66]	0.18 [0.16−0.20]	0.91 [0.83−0.99]	0.23 [0.18−0.28]
C_{R4}	0.55 [0.48−0.63]	0.35 [0.33−0.37]	0.44 [0.43−0.44]	1.00 [1.00−1.00]	0.37 [0.33−0.41]	1.26 [1.03−1.55]
C_{R6}	0.43 [0.35−0.51]	0.83 [0.78−0.88]	0.79 [0.78−0.82]	0.43 [0.42−0.43]	0.54 [0.50−0.59]	0.91 [0.75−1.09]
C_{R7}	0.39 [0.30−0.48]	0.91 [0.85−0.99]	0.80 [0.77−0.84]	0.38 [0.37−0.39]	0.45 [0.41−0.50]	0.99 [0.82−1.20]

References

Agrawal, A.A. (1998). Algal defense, grazers, and their interactions in aquatic trophic cascades. *Acta Oecologica*, 19: 331–337.

Barnett, A.J. et al. (2007). Functional diversity of crustacean zooplankton communities: towards a trait–based classification. *Freshwater Biology*, 52: 796–813.

Barreiro, A. and Hairston, N.G. (2013). The influence of resource limitation on the allelopathic effect of *Chlamydomonas reinhardtii* on other unicellular freshwater planktonic organisms. *Journal of Plankton Research*, 35: 1339–1344.

Barrett, R.D. and Schluter, D. (2008). Adaptation from standing genetic variation. *Trends in Ecology and Evolution*, 23: 38–44.

Bateman, A. et al. (2014). When to defend: antipredator defenses and the predation sequence. *The American Naturalist*, 183: 847–855.

Becks, L. et al. (2010). Reduction of adaptive genetic diversity radically alters eco-evolutionary community dynamics. *Ecology letters*, 13: 989–997.

Becks, L. et al. (2012). The functional genomics of an eco-evolutionary feedback loop: linking gene expression, trait evolution, and community dynamics. *Ecology Letters*, 15: 492–501.

Bennett, W.N. and Boraas, M.E. (1989). Comparison of population dynamics between slow- and fast-growing strains of the rotifer *Brachionus calyciflorus* pallas in continuous culture. *Oecologia*, 81: 494–500

Bernardes, J. et al. (2021). The evolution of convex trade-offs enables the transition towards multicellularity. *Nature Communication*, 12: 4222.

Bi, R. and Sommer, U. (2020). Food quantity and quality interactions at phytoplankton-zooplankton interface: chemical and reproductive responses in a calanoid copepod. *Frontiers in Marine Science*, 7: 274.

Breiman, L. (2001), Random forests. *Machine Learning*, 45: 5−32.

Brose, U. et al. (2005). From food webs to ecological networks: linking non-linear trophic interactions with nutrient competition. In: *Dynamic food webs* (eds. de Ruiter, P., Wolters, V. and Moore, J.), *Academic Press*, Burlington, USA, 27−36.

Bruggeman, J. (2011). A phylogenetic approach to the estimation of phytoplankton traits. *Journal of Phycology*, 47: 52−65.

Cadier, M. et al. (2019). Competition–defense tradeoff increases the diversity of microbial plankton communities and dampens trophic cascades. *Oikos*, 128: 1027–1040.

Colina, M. et al. (2016). A trait–based approach to summarize zooplankton–phytoplankton interactions in freshwaters. *Hydrobiologia*, 767: 221–233.

Cortez, M.H. (2016). How the magnitude of prey genetic variation alters predator-prey eco-evolutionary dynamics. *The American Naturalist*, 188: 329–341.

DeMott, W.R. et al. (2010). Ontogeny of digestion in Daphnia: implications for the effectiveness of algal defenses. *Ecology*, 91: 540–548.

Edwards, K.F. et al. (2011). Evidence for a three-way trade-off between nitrogen and phosphorus competitive abilities and cell size in phytoplankton. *Ecology*, 92: 2085–2095.

Edwards, K.F. et al. (2013). Functional traits explain phytoplankton community structure and seasonal dynamics in a marine ecosystem. *Ecology Letters*, 16: 53–63.

Ehrlich, E. and Gaedke, U. (2018). Not attackable or not crackable. How pre- and post-attack defenses with different competition costs affect prey coexistence and population dynamics. *Ecology and Evolution*, 8: 6625–6637.

Ehrlich, E. et al. (2017). Trait–fitness relationships determine how trade-off shapes affect species coexistence. *Ecology*, 98: 3188–3198.

Ehrlich, E. et al. (2020). The shape of a defense-growth trade-off governs seasonal trait dynamics in natural phytoplankton. *The ISME Journal*, 14: 1451–1462.

Ellner, S.P. and Becks, L. (2011). Rapid prey evolution and the dynamics of two-predator food webs. *Theoretical Ecology*, 4: 133–152.

Fischer, B.B. et al. (2014). Phenotypic plasticity influences the eco-evolutionary dynamics of a predator–prey system. *Ecology*, 95: 3080–3092.

Fleischer, S.R. et al. (2018). Pick your trade-offs wisely: Predator-prey eco-evo dynamics are qualitatively different under different trade-offs. *Journal of Theoretical Biology*, 456: 201–212.

Frickel, J. et al. (2017). Rapid evolution of hosts begets species diversity at the cost of intraspecific diversity. *Proceedings of the National Academy of Sciences of the USA*, 114: 11193–11198.

Friedrichs, L. et al. (2013). Size and biomechanic properties of diatom frustules influence food uptake by copepods. *Marine Ecology Progress Series*, 481: 41–51.

Fuller, R.C. et al. (2005). How and when selection experiments might actually be useful. Integrative and Comparative Biology, 45: 391–404.

Fussmann, G.F. et al. (2000). Crossing the Hopf bifurcation in a live predator-prey system. *Science*, 290: 1358–1360.

Fussmann, G.F. et al. (2003). Evolution as a critical component of plankton dynamics. *Proceedings of the Royal Society B*, 207: 1015–1022.

Fry, J.D. (2003). Detecting ecological trade-offs using selection experiments. *Ecology*, 84: 1672–1678.

Gibert, J.P. and Brassil, C. (2014). Individual phenotypic variation reduces interaction strengths in a consumer–resource system. *Ecology and Evolution*, 4: 3703–3713.

Gilbert, B. et al. (2014). A bioenergetic framework for the temperature dependence of trophic interactions. *Ecology Letters*, 17: 902–914.

Hairston, N.G. et al. (2005). Rapid evolution and the convergence of ecological and evolutionary time. *Ecology Letters*, 8: 1114–1127.

643 Halsey, K.H. and Jones, B.M. (2015). Phytoplankton strategies for photosynthetic energy allocation.
644 *Annual Review of Marine Science*, 7: 265–297.

645 Hammill, E. et al. (2010). Predator functional response changed by induced defenses in prey. *The*
646 *American Naturalist*, 176: 723–731.

647 Harvey, E.L. et al. (2015). Consequences of strain variability and calcification in Emiliania huxleyi on
648 microzooplankton grazing. *Journal of Plankton Research*, 37: 1137–1148.

649 Heinen, M. (1999) Analytical growth equations and their Genstat 5 equivalents. *Netherlands Journal of*
650 *Agricultural Science*, 47: 67–89.

651 Herrman, R.J. and Becks, L. (2022). Change in prey genotype frequency rescues predator from
652 extinction. *BioRxiv*, https://doi.org/10.1101/2022.04.19.487766.

653 Hessen, D.O. and Van Donk, E. (1993). Morphological-changes in Scenedesmus induced by substances
654 released from Daphnia. *Archiv fur Hydrobiologie*, 127: 129–140.

655 Holling, C.S. (1959). Some characteristics of simple types of predation and parasitism. *Canadian*
656 *Entomologist*, 91: 385–398.

657 Holling, C.S. (1965). The functional response of predators to prey density. *Memoirs of the*
658 *Entomological Society of Canada*, 45: 1–60.

659 Huang, W. et al. (2018). Dynamical trade-offs arise from antagonistic coevolution and decrease
660 intraspecific diversity. *Nature Communication*, 8: 2059.

661 Hubbell, S.P. (2005). Neutral theory in community ecology and the hypothesis of functional
662 equivalence. *Functional Ecology*, 19: 166–172.

663 Hudson, P.J. et al. (2002). Trophic interactions and population growth rates: describing patterns and
664 identifying mechanisms. *Philosophical Transactions of the Royal Society B*, 357: 1259–1271.

665 Ivlev, V.S. (1955). Experimental ecology of the feeding of fishes. *Pischepromizdat*, Moscow, 302 p.
666 (Translated from Russian by D. Scott, *Yale University Press*, New Haven, 1961).

667 Jeschke, J.M. et al. (2002). Pedator functional responses: discriminating between handling and digesting
668 prey. *Ecological Monograph*, 72: 95–112.

669 Jeschke, J.M. et al. (2004). Consumer–food systems: why type I functional responses are exclusive to
670 filter feeders. *Biological Reviews*, 79: 337–349.

671 Jessup, C.M. and Bohannan, B.J. (2008). The shape of an ecological trade-off varies with environment.
672 *Ecology Letters*, 11: 947–959.

673 Jochimsen, M.C. et al. (2013). Compensatory dynamics and the stability of phytoplankton biomass
674 during four decades of eutrophication and oligotrophication. *Ecology Letters*, 16: 81–89.

675 Jones, L.E. and Ellner, S.P. (2007). Effects of rapid prey evolution on predator-prey cycles. *Journal of*
676 *Mathematical Biology*, 55: 541–573.

677 Jones, L.E. et al. (2009). Rapid contemporary evolution and clonal food web dynamics. *Philosophical*
678 *Transactions of the Royal Society B*, 364: 1579–1591.

679 Jonsson, T. et al. (2010). Trophic interactions affect the population dynamics and risk of extinction of
680 basal species in food webs. *Ecological Complexity*, 7: 60−68.

681 Jost, J.L. et al. (1973). Microbial food chains and food webs. *Journal of Theoretical Biology*, 41: 461–
682 484.

683 Kalinoski, R.M. and DeLong, J.P. (2016). Beyond body mass: how prey traits improve predictions of
684 functional response parameters. *Oecologia*, 180: 543–550.

685 Kasada, M. et al. (2014). Form of an evolutionary trade-off affects eco-evolutionary dynamics in a
686 predator–prey system. *Proceedings of the National Academy of Sciences of the USA*, 111: 16035–16040.

687 Kassen, R. (2002). The experimental evolution of specialists, generalists, and the maintenance of
688 diversity. *Journal of Evolutionary Biology*, 15:173–190.

689 Kiørboe, T. (2008). A mechanistic approach to plankton ecology. *Princeton University Press*, Princeton:
690 224 p.

691 Kiørboe, T. et al. (2016). Foraging mode and prey size spectra of suspension-feeding copepods and other
692 zooplankton. *Marine Ecology Progress Serie*, 558: 15–20

693 Kiørboe, T. et al. (2017). Adaptive feeding behavior and functional responses in zooplankton. *Limnology*
694 *and Oceanography*, 63: 308–321.

695 Klausmeier, C.A. et al. (2004). Optimal nitrogen-to-phosphorus stoichiometry of phytoplankton.
696 *Nature*, 429: 171–174.

697 Kneitel, J.M. and Chase, J.M. (2004). Trade-offs in community ecology: linking spatial scales and
698 species coexistence. *Ecology Letters*, 7: 69–80.

699 Kolb, A. and Strom, S. (2013). An inducible antipredatory defense in haploid cells of the marine
700 microalga Emiliania huxleyi (Prymnesiophyceae). *Limnology and Oceanography*, 58: 932–944.

701 Litchman, E. (2007). Resource competition and the ecological success of phytoplankton. In: Evolution
702 of primary producers in the sea (eds. Falkowski, P.G. and Knoll, A.H.). *Elsevier*, New York, USA,
703 351−375.

704 Litchman, E. and Klausmeier, C.A. (2008). Trait–based community ecology of phytoplankton. *Annual*
705 *Review of Ecology Evolution and Systematics*, 39: 615–639.

706 Litchman, E. et al. (2007). The role of functional traits and trade-offs in structuring phytoplankton
707 communities: scaling from cellular to ecosystem level. *Ecology Letters*, 10: 1170–1181.

708 Litchman, E. et al. (2009). Contrasting size evolution in marine and freshwater diatoms. *Proceedings of*
709 *the National Academy of Sciences of the USA*, 106: 2665–2670.

710 Litchman, E. et al. (2010). Linking traits to species diversity and community structure in phytoplankton.
711 *Hydrobiologia*, 653:15–28.

712 Litchman, E. et al. (2013). Trait–based approaches to zooplankton communities. *Journal of Plankton*
713 *Research*, 35: 473–484.

714 Litchman, E. et al. (2015). Microbial resource utilization traits and trade-offs: implications for
715 community structure, functioning, and biogeochemical impacts at present and in the future. *Frontiers in*
716 *Microbiology*, 6: 1–10.

Long, J.D. et al. (2007). Chemical cues induce consumer-specific defenses in a bloom-forming marine phytoplankton. *Proceedings of the National Academy of Sciences of the USA*, 104: 10512–10517.

Lürling, M. (2006). Palmelloids formation in Chlamydomonas reinhardtii: defence against rotifer predators? *International Journal of Limnology*, 42: 65−72.

Lürling, M. (2020). Grazing resistance in phytoplankton. *Hydrobiologia*, 848: 237–249.

Lürling, M. and Van Donk, E. (1996). Zooplankton-induced unicell-colony transformation in Scenedesmus acutus and its effect on growth of herbivore Daphnia. *Oecologia*, 108, 432–437.

Lürling, M. and Van Donk, E. (2000). Grazer-induced colony formation in Scenedesmus: are there costs to being colonial? *Oikos*, 88: 111–118.

Malerba, M.E. et al. (2018). Do larger individuals cope with resource fluctuations better? An artificial selection approach. *Proceedings of the Royal Society B*, 285: 20181347.

Modenutti, B. et al. (2003). Impact of different zooplankton structures on the microbial food web of a South Andean oligotrophic lake. *Acta Oecologica*, 24: 289–298.

Monod, J. (1950). La technique de culture continue: Théorie et applications. *Annales de l'Institut Pasteur*, 79 : 390–410.

Mullin, M.M. et al. (1975). Ingestion by planktonic grazers as a function of food concentration. *Limnology and Oceanography*, 20: 259–262.

Murdoch, W.W. et al. (2003). Consumer–Resource Dynamics. *Princeton University Press*, Princeton: 464 p.

Pančić, M. and Kiørboe, T. (2018). Phytoplankton defence mechanisms: traits and trade-offs. *Biological Reviews*, 93: 1269–1303.

Paine, C.E. et al. (2012). How to fit nonlinear plant growth models and calculate growth rates: an update for ecologists. *Methods in Ecology and Evolution*, 3: 245–256.

Persson, A. et al. (2001). Effects of enrichment on simple aquatic food webs. *The American Naturalist*, 6: 664−669.

Petchey, O.L. et al. (2008). Size, foraging, and food web structure. *Proceedings of the National Academy of Sciences of the USA*, 105: 4191-4196.

Pondaven, P. et al. (2007). Grazing-induced changes in cell wall silicification in a marine diatom. *Protist*, 158: 21–28.

Quintana, X.D. et al. (2015). Predation and competition effects on the size diversity of aquatic communities. *Aquatic Sciences*, 77: 45–57.

R Development Core Team. 2020. R: A language and environment for statistical computing. R Foundation for Statistical Computing, Vienna, Austria.

Rall, B.C. et al (2012). Universal temperature and body-mass scaling of feeding rates. *Philosophical Transaction of the Royal Society B*, 367: 2923–2934.

Ratcliff, W.C. et al. (2013). Experimental evolution of an alternating uni- and multicellular life cycle in Chlamydomonas reinhardtii. *Nature Communications*, 4: 2742.

Reynolds, C.S. (2006). Ecology of phytoplankton. *Cambrige University Press*, New York: 1–535.

Rip, J.M. and McCann, K.S. (2011). Cross-ecosystem differences in stability and the principle of energy flux. *Ecology Letters*, 14: 733–740.

Smith, S.L. et al. (2014). Sizing-up nutrient uptake kinetics: combining a physiological trade-off with size-scaling of phytoplankton traits. *Marine Ecology Progress Series*, 511: 33–39.

Smith, S.L. et al. (2016). Phytoplankton size-diversity mediates an emergent trade-off in ecosystem functioning for rare versus frequent disturbances. *Scientific Reports*, 6: 34170.

Sommer, U. (2008). Trophic cascades in marine and freshwater plankton. *International Review of Hydrobiology*, 93: 506–516.

Sommer, U. et al. (2012). Beyond the Plankton Ecology Group (PEG) Model: mechanisms driving plankton succession. *Annual Review of Ecology Evolution and Systematics*, 43: 429–448.

Stearns, C.S. (1989). Trade-offs in life-history evolution. *Functional Ecology*, 3: 259−268.

Strauss, S.Y. et al. (2002). Direct and ecological costs of resistance to herbivory. *Trends in Ecology and Evolution*, 17: 278–285.

Strzepek, R.F. and Harrison, P.J. (2004). Photosynthetic architecture differs in coastal and oceanic diatoms. *Nature*, 431: 689–692.

Sunda, W.G. and Hardison, D.R. (2010). Evolutionary tradeoffs among nutrient acquisition, cell size, and grazing defense in marine phytoplankton promote ecosystem stability. *Marine Ecology Progress Series*, 40: 63–76.

Thackeray, S.J. (2008). Long-term change in the phenology of spring phytoplankton: species-specific responses to nutrient enrichment and climatic change. *Functional Ecology*, 96, 523–535.

Thébault, E. and Loreau, M. (2005). Trophic interactions and the relationship between species diversity and ecosystem stability. *The American Naturalist*, 166: 95−114.

Theodosiou, L. et al. (2019). The role of stressors in altering eco-evolutionary dynamics. *Functional Ecology*, 33: 73–83.

Tirok, K. and Gaedke, U. (2010). Internally driven alternation of functional traits in a multispecies predator–prey system. *Ecology*, 91: 1748–1762.

Turner, J.T. (2002). Zooplankton fecal pellets, marine snow and sinking phytoplankton blooms. *Aquatic Microbial Ecology*, 27: 57–102.

Turner, J.T. (2015). Zooplankton fecal pellets, marine snow, phytodetritus and the ocean's biological pump. *Progress in Oceanography*, 130: 205–248.

Våge, S. et al. (2014). Optimal defense strategies in an idealized microbial food web under trade-off between competition and defense. *PloS One*, 9: e101415

Van Donk, E. and Hessen, D.O. (1993). Grazing resistance in nutrient-stressed phytoplankton. *Oecologia*, 93: 508−511.

789 Van Donk, E. et al. (1999). Consumer-induced changes in phytoplankton: inducibility, costs, benefits
790 and impacts on grazers. In: The ecology and evolution of inducible defenses (eds. Tollrian R. and
791 Harvell, C.D.). *Princeton University Press*, Princeton, USA, 89−110.

792 Van Donk, E. et al. (2011). Induced defences in marine and freshwater phytoplankton: a review.
793 *Hydrobiologia*, 668: 3–19.

794 Verschoor, A.M. et al. (2004). Inducible colony formation within the Scenedesmaceae: adaptive
795 responses to infochemicals from two different herbivore taxa. *Journal of Phycology*, 40: 808–814.

796 Ward, B.A. et al. (2017). The size dependence of phytoplankton growth rates: a trade-off between
797 nutrient uptake and metabolism. *The American Naturalist*, 189: 170–177.

798 Weiss, L. et al. (2012). The taste of predation and the defences of prey. In: Chemical ecology in aquatic
799 systems (eds. Brönmark, C. and Hansson, L.A.). *Oxford University Press*, Oxford, UK, 111–126.

800 Yamamichi, M. and Miner, B.E. (2015). Indirect evolutionary rescue: prey adapts, predator avoids
801 extinction. *Evolutionary Applications*, 8: 787–795.

802 Yamamichi, M. et al. (2011). Comparing the effects of rapid evolution and phenotypic plasticity on
803 predator-prey dynamics. *American Naturalist*, 178: 287–304.

804 Yoshida, T. et al. (2003). Rapid evolution drives ecological dynamics in a predator–prey system. *Nature*,
805 424: 303−306.

806 Yoshida, T. et al. (2004). Evolutionary trade-off between defence against grazing and competitive ability
807 in a simple unicellular alga, Chlorella vulgaris. *Proceedings of the Royal Society B*, 271: 1947–1953.

808 Yoshida, T. et al. (2007). Cryptic population dynamics: rapid evolution masks trophic interactions. *PloS*
809 *Biology*, 5: e235.

810 Yoshiyama, K. and Klausmeier, C.A. (2008). Optimal cell size for resource uptake in fluids: a new
811 facet of resource competition. *The American Naturalist*, 171: 59−70.